Phosphorylation of the Human Fhit Tumor Suppressor on Tyrosine 114 in *Escherichia coli* and Unexpected Steady State Kinetics of the Phosphorylated Forms†

Preston N. Garrison,‡ Angela K. Robinson,‡ Yuri Pekarsky,§ Carlo M. Croce,§ and Larry D. Barnes*,‡

Department of Biochemistry, University of Texas Health Science Center, San Antonio, Texas 78229-3900, and Comprehensive Cancer Center, The Ohio State University, Columbus, Ohio 43210

Received November 2, 2004; Revised Manuscript Received February 9, 2005

ABSTRACT: The human tumor suppressor Fhit is a homodimeric histidine triad (HIT) protein of 147 amino acids which has Ap_3A hydrolase activity. We have recently discovered that Fhit is phosphorylated in vivo and is phosphorylated in vitro by Src kinase [Pekarsky, Y., Garrison, P. N., Palamarchuk, A., Zanesi, N., Aqeilan, R. I., Huebner, K., Barnes, L. D., and Croce, C. M. (2004) *Proc. Natl. Acad. Sci. U.S.A. 101*, 3775−3779]. Now we have coexpressed Fhit with the elk tyrosine kinase in *Escherichia coli* to generate phosphorylated forms of Fhit. Unphosphorylated Fhit, Fhit phosphorylated on one subunit, and Fhit phosphorylated on both subunits were purified to apparent homogeneity by column chromatography on anion-exchange and gel filtration resins. MALDI-TOF and HPLC-ESI tandem mass spectrometry of intact Fhit and proteolytic peptides of Fhit demonstrated that Fhit is phosphorylated on Y^{114} on either one or both subunits. Monophosphorylated Fhit exhibited monophasic kinetics with K_m and k_{cat} values ∼2- and ∼7-fold lower, respectively, than the corresponding values for unphosphorylated Fhit. Diphosphorylated Fhit exhibited biphasic kinetics. One site had K_m and k_{cat} values ∼2- and ∼140-fold lower, respectively, than the corresponding values for unphosphorylated Fhit. The second site had a K_m ∼60-fold higher and a k_{cat} ∼6-fold lower than the corresponding values for unphosphorylated Fhit. The unexpected kinetic patterns for the phosphorylated forms suggest the system may be enzymologically novel. The decreases in the values of K_m and k_{cat} for the phosphorylated forms in comparison to those of unphosphorylated Fhit favor the formation and lifetime of the Fhit−Ap_3A complex, which may enhance the tumor suppressor activity of Fhit.

Human Fhit[1] is a 147-amino acid protein which forms a homodimer containing two active sites and hydrolyzes Ap_3A to AMP and ADP. It is encoded by the *FHIT* gene that spans the FRA3B fragile site at chromosome 3p14.2 (*1*, *2*). Observation of hemi- and homozygous deletions in the *FHIT* locus in cell lines derived from a number of different tumors and observation of aberrant transcripts in different types of primary tumors led to the proposal that Fhit is a tumor suppressor (reviewed in refs *3*−*7*). The strongest evidence that Fhit is a tumor suppressor is (1) stable transfection of *FHIT*(−) cancer cell lines with *FHIT* induced apoptosis and suppressed tumorigenicity of the cells in nude mice (*8*), (2) suppression of tumor cell growth both in vivo and in vitro by adenovirus vector-mediated overexpression of *FHIT* (*9*), (3) increased susceptibility to induced and spontaneous tumors in *FHIT* knockout mice (*10*), and (4) prevention of inducible forestomach tumors in *FHIT*(+/−) mice by oral adminstration of adeno and adeno-associated *FHIT* viruses (*11*, *12*). Overexpression of the Fhit protein in malignant cells lacking endogenous Fhit causes cell cycle arrest and induces apoptosis as measured by DNA strand breaks and activation of particular caspases (*13*, *14*).

Sequence comparisons and structure determination by X-ray diffraction (*15*−*17*) have revealed that Fhit and its orthologs constitute a eukaryotic-specific branch of the histidine triad (HIT) [or GAFH (*4*)] superfamily of nucleotidyl transferases and hydrolases (*18*). All the eukaryotic genomes sequenced to date contain a *FHIT* gene. The superfamily is characterized by a HxHx(H/Q) motif at the active site. All characterized members of the superfamily catalyze a nucleotidyl transfer or hydrolysis which depends on formation of a covalent nucleoside monophosphate−histidine intermediate at the central histidine of the triad (H^{96} in human Fhit). Fhit and its orthologs that have been tested all hydrolyze Ap_3A, Ap_4A, or both (*19*−*22*). The hydrolytic

† Supported by NSF Grant MCB-9982645 (to L.D.B.) and NCI Grants CA77738 and CA56036 (to C.M.C.).

* To whom correspondence should be addressed: Department of Biochemistry, University of Texas Health Science Center, 7703 Floyd Curl Dr., San Antonio, TX 78229-3900. Telephone: (210) 567-3730. Fax: (210) 567-6595. E-mail: barnesl@uthscsa.edu.

‡ University of Texas Health Science Center.

§ The Ohio State University.

[1] Abbreviations: Fhit, fragile histidine triad protein from humans; *FHIT*, gene encoding Fhit; HIT, histidine triad; Ap_3A, diadenosine 5′,5‴-P^1,P^3-triphosphate; Ap_4A, diadenosine 5′,5‴-P^1,P^4-tetraphosphate; MALDI-TOF, matrix-assisted laser desorption ionization time-of-flight; ESI, electrospray ionization; HPLC, high-performance liquid chromatography; CID, collision-induced dissociation; GalT, galactose-1-phosphate uridylyl transferase from *E. coli*; GAFH, GalT, Ap_4A phosphorylase, Fhit, Hint; IPTG, isopropyl β-D-thiogalactopyranoside; LB, Luria−Bertani; PMSF, phenylmethanesulfonyl fluoride; HEPES, *N*-(2-hydroxyethyl)piperazine-*N*′-ethanesulfonic acid; TFA, trifluoroacetic acid.

10.1021/bi047670s CCC: $30.25
Published on Web 03/29/2005

activity of Fhit is lost almost completely when H^{96} is changed to asparagine (*15*). In a single-turnover reaction with Ap_3A, FhitH^{96}N is unable to release ADP, and thus presumably cannot form the covalent intermediate (*15*). The hydrolysis of an Ap_3A analogue by Fhit proceeds with retention of stereochemical configuration at the α-phosphate, as expected for a double-displacement mechanism (*23*). Recently, Frey and co-workers provided direct evidence for such a mechanism by trapping 11% of the enzyme in the steady state as an adenylyl−Fhit intermediate and chemical rescue of H^{96}G-Fhit, which is incapable of forming the covalent intermediate, using imidazole or AMP−imidazole (*24*).

The results above indicate that Fhit has evolved as a nucleotide hydrolytic enzyme that is similar to others in its structure class. However, a mystery arises from the fact that the FhitH^{96}N mutant, which has a normal structure but almost no enzyme activity (*15*, *20*), is nonetheless active as a tumor suppressor (*8*, *25*). Because this mutated protein binds Ap_3A well, it has been proposed that a nucleotide-bound form of Fhit may be the active species in tumor suppression in a manner analogous to that of GTP binding proteins (*15*). Recently, Trapasso et al. have provided strong support for this model (*26*). They made a series of mutant Fhit forms with increased K_m values for Ap_3A, decreased k_{cat} values, or both, and measured their effectiveness in inducing apoptosis in Fhit(−) cell lines when expressed from an adenovirus construct. The level of induction of apoptosis was decreased only with an increased K_m, with no effect of changes in k_{cat}.

Recently, we have shown that Fhit is phosphorylated in vivo in normal human tissues and in human embryonic kidney cells and in vitro by Src kinase (*27*). Tyrosine 114 is phosphorylated both in vivo and in vitro (*27*). This was the first report about phosphorylation of Fhit, and it likely provides a critical element in determining the biochemical mechanism of Fhit's function as a tumor suppressor. Here we report on phosphorylation of human Fhit in *Escherichia coli* and the purification, mass spectrometric analyses, and the unexpected kinetic properties of the phosphorylated forms of Fhit.

EXPERIMENTAL PROCEDURES

Materials. Ap_3A was custom-labeled with tritium by Moravek Biochemicals, Inc. *E. coli* strain TKB1 was purchased from Statagene. DEAE-Sephacel, Sephadex G-75 superfine, and QAE-Sepharose resins were purchased from Sigma. Electrophoresis reagents were from Bio-Rad. Sequencing-grade, modified porcine trypsin was from Promega, and sequencing-grade endoproteinase Glu-C (V_8 protease) from *Staphylococcus aureus* was from Roche Applied Science.

Transformation and Protein Expression. We transformed *E. coli* TKB1 (Stratagene), a strain containing a plasmid with the *elk* broad-specificity tyrosine kinase gene, with pSGA02*FHIT* (*28*). Transformed cells were grown in LB medium containing ampicillin (100 μg/mL) and tetracycline (12.5 μg/mL) at 37 °C to an OD of ∼0.8 at 600 nm. Then protein expression was induced with 1 mM IPTG at 25 °C for 16−18 h. We found that these growth and induction conditions were sufficient for expression of both Fhit and the tyrosine kinase and that it was not necessary to induce expression of the tyrosine kinase in defined medium with indoleacrylic acid (Stratagene protocol manual). Sixteen to seventeen grams of wet weight of the bacterial cell pellet was harvested from 5 L of cells. We also expressed unphosphorylated Fhit in *E. coli* SG100 (*29*) as previously described (*28*).

Protein Purification and Electrophoresis. Cell pellets were suspended in 50 mM HEPES (pH 6.8) and 10% glycerol containing 0.5 mM PMSF, 1.1 μM leupeptin, and 0.7 μM pepstatin at a ratio of 3 mL per gram of wet weight. The cell suspension was sonicated on ice for 3 × 30 s using an Ultrasonic Processor sonicator at a power setting of 6 on a macrotip. The resulting homogenate was centrifuged at 43000*g* at 4 °C for 30 min to obtain a crude supernatant fraction. Crude supernatant fractions from the two transformed strains were dialyzed in 25 mM HEPES (pH 6.8) and 10% glycerol containing 0.5 mM PMSF. Typically, a dialyzed crude supernatant fraction was subjected to column chromatography on DEAE-Sephacel resin equilibrated in 25 mM HEPES (pH 6.8) and 10% glycerol and eluted with a linear gradient from 0 to 0.3 M NaCl. Fractions were pooled on the basis of their Ap_3A hydrolase activity and concentrated in an Amicon stirred cell with a PM-10 membrane under N_2. The concentrated DEAE-Sephacel fraction was applied to a Sephadex G-75 gel filtration column equilibrated in 50 mM HEPES (pH 6.8) and 10% glycerol. Fractions containing the dimeric form of Fhit were pooled and applied to a column of QAE-Sepharose resin equilibrated in 50 mM HEPES (pH 6.8) and 10% glycerol. Proteins were eluted with a linear gradient of 0 to 0.15 M NaCl. Fractions were pooled on the basis of their Ap_3A hydrolase activity and their gel electrophoretic pattern. Pooled fractions were dialyzed in 50 mM HEPES (pH 6.8) and 10% glycerol and then concentrated in an Amicon stirred cell with a PM-10 membrane under N_2. Proteins were subjected to electrophoresis on 15% polyacrylamide−SDS gels (*30*, *31*) and stained with Coomassie blue.

Mass Spectrometry. MALDI-TOF mass spectra were acquired on an Applied Biosystems Voyager-Elite mass spectrometer using a matrix of sinapinic acid (saturated solution in 50% acetonitrile containing 0.1% TFA). Fhit samples were subjected to reversed-phase chromatography on a C18 matrix (ZipTips from Millipore, Inc.) and eluted with 50% acetonitrile and 0.1% TFA. One microliter of eluate was spotted on the MALDI target, overlayed with the matrix, and allowed to dry at room temperature. Each MALDI-TOF mass spectrum represents the average of 64 laser shots acquired in linear mode over a mass range of *m*/*z* 4000−28000, using delayed extraction and positive ion detection. Spectra were processed by the smoothing and noise reduction protocols of the data system software. Close external calibration based on myoglobin was employed.

HPLC−ESI tandem mass spectra were acquired on a Thermo Finnigan LCQ Classic ion trap mass spectrometer connected via a microspray interface to a Michrom BioResources MAGIC 2002 micro HPLC system. For on-line HPLC separations, a New Objective PicoFrit was packed to 10 cm with Vydac 218MSB5 (5 μm, 300 Å) C18 reversed-phase matrix. HPLC conditions were as follows: mobile phase A, 0.5% acetic acid and 0.005% TFA; mobile phase B, 90% acetonitrile, 0.5% acetic acid, and 0.005% TFA; gradient, from 2 to 72% B over the course of 30 min; initial flow rate, approximately 0.4 μL/min. ESI-MS/MS conditions

were as follows: electrospray voltage of 3 kV, heated capillary temperature of 175 °C, isolation window for CID of 2.5, relative collision energy of 35%, and spectral acquisition in centroid mode. For initial on-line HPLC−ESI-MS/MS experiments, each scan segment consisted of a survey scan followed by acquisition of CID mass spectra of the four most abundant ions in the survey scan above a selected threshold. Subsequent HPLC−ESI-MS/MS analyses employed a targeted scan strategy in which the specific *m*/*z* values for Fhit proteolytic peptides of interest were monitored.

Diphosphorylated Fhit was subjected to proteolysis by trypsin and by endoproteinase Glu-C (V_8 protease) for 16−18 h at ~25 °C in 40 mM ammonium bicarbonate (pH 7.6) and in 25 mM ammonium acetate (pH 4.0), respectively (*32*). The resulting peptides were analyzed by ESI mass spectrometry, as described above, to identify the specific phosphorylated residue(s).

Enzymatic Assay. We assayed the Ap_3A hydrolase activity of Fhit by assessing the hydrolysis of [^{3}H]Ap_3A. For the assay of column fractions during purification, samples were incubated with 100 μM [^{3}H]Ap_3A in 50 mM HEPES (pH 6.8) and 0.5 mM $MnCl_2$ at 37 °C for 10 min. For determination of kinetic parameters, purified Fhit samples were incubated under the same conditions with different concentrations of [^{3}H]Ap_3A ranging from 0.05 to 500 μM, depending upon the particular unphosphorylated or phosphorylated form of Fhit. Reaction products were separated from the residual substrate by chromatography on a boronate-derivatized resin (*33*). For each of the different forms of Fhit, the activity was a linear function of both time and mass of the protein. Values of the kinetic parameters were calculated by a weighted, least-squares fitting of the data to the Michaelis−Menten equation, with corrections whenever the hydrolysis of substrate exceeded 10% (*34*), except in the case of diphosphorylated Fhit where the kinetics were biphasic and the data were fitted to a two-component Michaelis−Menten equation. Data also were analyzed using Hanes and Eadie−Hofstee plots to confirm the monophasic and biphasic kinetics for the different phosphorylated forms.

RESULTS

Purification of Phosphorylated Forms of Human Fhit from an E. coli Expression System. Human Fhit was coexpressed in *E. coli* TKB1 (Stratagene) with the elk tyrosine kinase. Three forms of Fhit were purified by sequential column chromatography on DEAE-Sephacel, Sephadex G-75, and QAE-Sepharose resins as described in Experimental Procedures. Unphosphorylated Fhit was mostly resolved from the phosphorylated forms on DEAE-Sephacel, while the phosphorylated forms were not resolved from one another. Both unphosphorylated Fhit and the phosphorylated forms exhibited a high-molecular mass aggregate upon Sephadex G75 gel filtration chromatography, as previously reported for unphosphorylated Fhit (*28*). The dimeric unphosphorylated and phosphorylated forms of Fhit from their respective Sephadex G75 columns were subjected to chromatography on QAE-Sepharose resin. The monophosphorylated and diphosphorylated forms of Fhit were well resolved from one another as well as from the residual unphosphorylated Fhit (carried over from the DEAE-Sephacel and Sephadex G-75 columns) on QAE-Sepharose (Figure 1). On the basis of the gel electrophoretic pattern (Figure 1 insert) and enzymatic activity of column fractions (Figure 1), appropriate fractions corresponding to the different forms of Fhit were pooled and concentrated for subsequent analyses. The chromatographic resolution of the different forms of Fhit on a preparative scale on QAE-Sepharose resin was similar to that observed previously on an analytical scale using a FPLC-MonoQ column for purified Fhit phosphorylated in vitro with Src kinase (see Figure 1 in ref *27*).

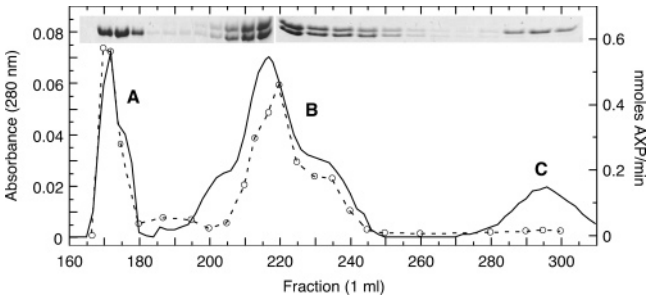

FIGURE 1: Chromatographic separation of unphosphorylated and phosphorylated forms of Fhit on QAE-Sepharose resin: (—) absorbance at 280 nm and (-O-O-) Ap_3A hydrolase activity. Labeled peaks are as follows: (A) unphosphorylated Fhit, (B) Fhit phosphorylated on one subunit, and (C) Fhit phosphorylated on both subunits. The inset shows SDS gel electrophoretic patterns of individual column fractions; 20 μL of each fraction designated by a circle was subjected to electrophoresis, and the gel was stained with Coomassie blue.

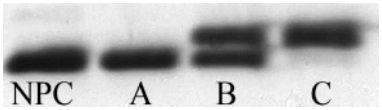

FIGURE 2: SDS−PAGE of purified Fhit fractions. NPC (nonphosphorylated control) is Fhit purified from the non-tyrosine-phosphorylating *E. coli* strain SG100. A−C, obtained by pooling and concentrating appropriate fractions from peaks labeled A−C in Figure 1, represent Fhit that is unphosphorylated, phosphorylated on one subunit, and phosphorylated on both subunits, respectively (data in Figure 3 confirm the identity of the phosphorylated forms of Fhit). Each lane contained ~2 μg of protein stained with Coomassie blue.

We judged unphosphorylated, monophosphorylated, and diphosphorylated Fhit isolated by this procedure to be at least 95% homogeneous based on the SDS gel electrophoretic patterns and mass spectrometry (Figures 2 and 3). Sixteen to seventeen grams of wet weight of cells yielded ~37, ~27, and ~7 mg of unphosphorylated, monophosphorylated, and diphosphorylated Fhit, respectively.

The three forms were analyzed on a SDS gel, and their pattern was compared to that of Fhit purified from the non-tyrosine-phosphorylating *E. coli* strain. The results are shown in Figure 2. We interpret fractions A−C in Figure 2 to be unphosphorylated Fhit, Fhit phosphorylated on one subunit, and Fhit phosphorylated on both subunits, respectively. Fraction B is unlikely to be a mixture of unphosphorylated and diphosphorylated Fhit based on the constant ratio of the two bands across the chromatographic peak and the chromatographic resolution of the three forms (Figure 1). The gel pattern in Figure 2 is the same as observed for the three forms of Fhit isolated from an in vitro Src kinase phosphorylation reaction (see Figure 2 in ref *27*).

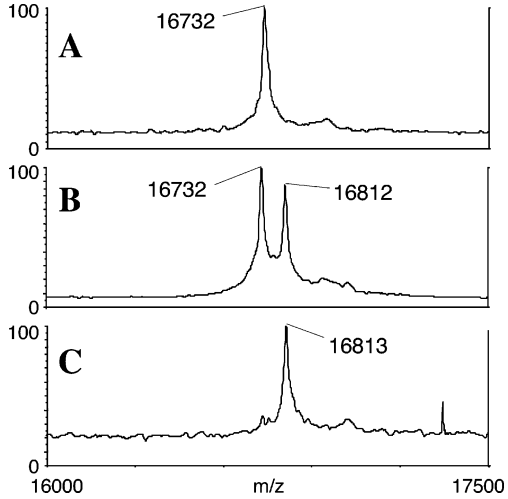

FIGURE 3: MALDI-TOF mass spectra of the purified forms of Fhit. (A) Fhit corresponding to fraction A in Figure 2 and unphosphorylated. (B) Fhit corresponding to fraction B in Figure 2 and phosphorylated on one residue in only one subunit. (C) Fhit corresponding to fraction C in Figure 2 and phosphorylated on one residue in both subunits. See the text for an explanation of phosphorylation data.

Mass Spectrometry of the Different Forms of Fhit. We analyzed the purified forms of Fhit, called fractions A−C in Figure 2, by mass spectrometry to determine their state of phosphorylation and to identify the phosphorylated residue(s). The MALDI-TOF spectrum of fraction A exhibited a single peak corresponding to a mass of 16 731 Da, the mass expected for the unphosphorylated Fhit monomer lacking the N-terminal methionine (Figure 3A). The spectrum for fraction B showed two peaks: one corresponding to a mass of 16 731 Da and one corresponding to a mass of 16 811 Da (Figure 3B). The mass increment of 80 Da indicated that one residue on a monomer was phosphorylated. The spectrum for fraction C exhibited a single peak corresponding to a mass of 16 812 Da (Figure 3C). Thus, the spectra are consistent with the conclusion that fraction A was unphosphorylated Fhit, that fraction B was Fhit phosphorylated on only one subunit, and that fraction C was Fhit phosphorylated on both subunits and that only one residue on each subunit was phosphorylated.

Fhit phosphorylated on both subunits (fraction C) was subjected to proteolysis by trypsin and endoproteinase Glu-C separately, and the resulting peptides were analyzed on an HPLC ion trap mass spectrometer to identify the specific phosphorylated residue(s). Among the tryptic peptides, only peptide 110−130 was phosphorylated, and the fragmentation pattern of the peptide was compatible only with Y^{114} being phosphorylated and not S^{112} or S^{128} (Figure 4). Analysis of Y^{145} was carried out with endoproteinase Glu-C-generated peptides, since the tryptic peptide containing Y^{145} was too small (four residues) for adequate recovery. No phosphorylated form of peptide 138−146 was detected. The only phosphorylated peptide that was detected was peptide 87−114 (data not shown). Thus, mass spectrometry data support the conclusion that fraction C was Fhit phosphorylated on Y^{114} on both subunits and only on Y^{114}.

Kinetic Parameters of the Different Phosphorylated Forms of Fhit. We assayed the Ap_3A hydrolase activity of unphosphorylated, monophosphorylated, and diphosphorylated Fhit and obtained the values for steady state kinetic parameters K_m, k_{cat}, and k_{cat}/K_m shown in Table l. Both unphosphorylated Fhit (Figure 5A) and monophosphorylated Fhit (Figure 5B) exhibited monophasic kinetics. Monophosphorylation of Fhit resulted in slower turnover of Ap_3A as indicated by a k_{cat} ~7-fold lower than the k_{cat} for unphosphorylated Fhit. The 2-fold decrease in K_m for monophosphorylated Fhit in comparison to that of unphosphorylated Fhit indicated an apparent tighter binding of Ap_3A upon monophosphorylation. Diphosphorylated Fhit exhibited biphasic kinetics (Figure 5C). One site had K_m and k_{cat} values ~2- and ~140-fold lower, respectively, than the corresponding values for unphosphorylated Fhit. The second site had a K_m ~60-fold higher and a k_{cat} ~6-fold lower than the corresponding values for unphosphorylated Fhit (Table 1).

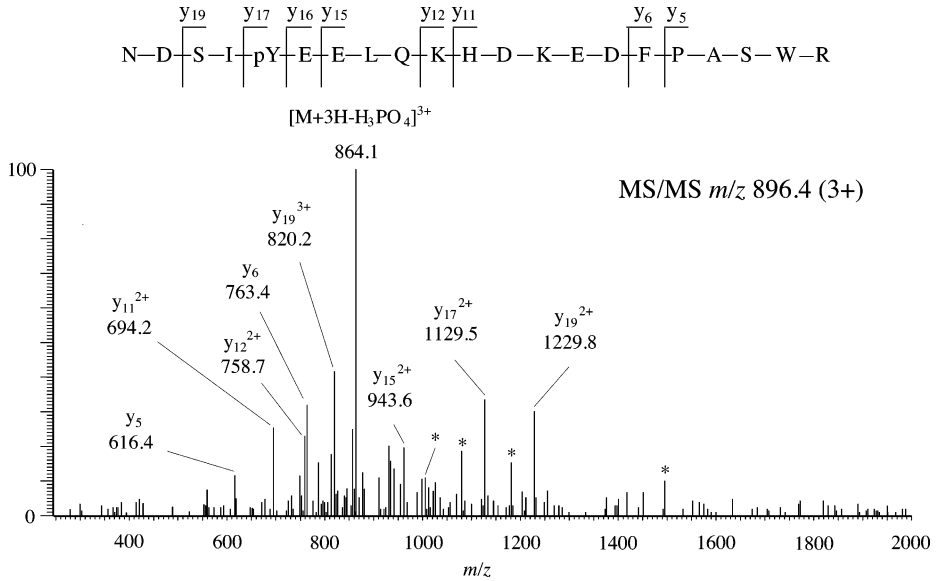

FIGURE 4: ESI tandem mass spectrum of diphosphorylated Fhit. Collision-induced dissociation mass spectrum of *m*/*z* 896.4 (3+ ion) of Fhit residues 110−130 (NDSIpY114EELQKHDKEDFPASWR). Selected C-terminal (y series) ions are labeled, with other sequence-informative ions denoted with asterisks. Diphosphorylated Fhit was subjected to proteolysis by trypsin, and the resulting peptides were analyzed by on-line HPLC−ESI-MS/MS as described in Experimental Procedures.

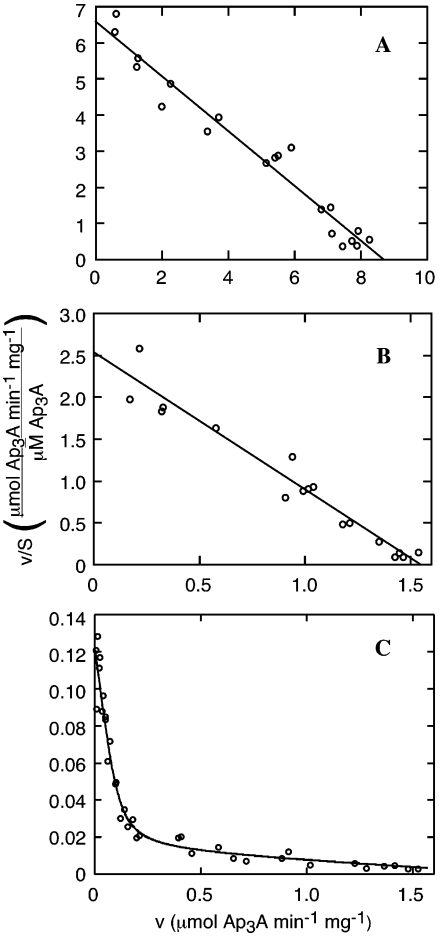

FIGURE 5: Eadie−Hofstee plots of representative kinetic data for the three forms of Fhit. The empty circles in each plot represent individual data points for duplicates in a representative assay for each form of Fhit. The data were directly fitted to the appropriate Michaelis−Menten equation to determine the kinetic parameters and plotted as v/S vs v to show the monophasic or biphasic nature of the kinetics. The fitted lines are derived from the direct fit kinetic parameters. (A) For unphosphorylated Fhit, the rate was measured as a function of substrate concentration from 0.1 to 20 μM. (B) For monophosphorylated Fhit, the rate was measured as a function of substrate concentration from 0.1 to 20 μM. (C) For diphosphorylated Fhit, the rate was measured as a function of substrate concentration from 0.05 to 500 μM. The data were directly fitted to a two-component Michaelis−Menten equation assuming equal numbers of independent catalytic sites for calculation of the values of K_m and V_{max} for both sites. Mean values of kinetic parameters for six assays for each form are presented in Table 1.

Table 1: Kinetic Parameters for Hydrolysis of Ap_3A by Different Forms of Fhit[a]

Fhit	K_m (μM)	k_{cat} (s^{-1} per monomer)	k_{cat}/K_m (s^{-1} M^{-1})
unphosphorylated	1.60 ± 0.19	2.74 ± 0.87	$(1.70 \pm 0.44) \times 10^6$
monophosphorylated	0.67 ± 0.14	0.38 ± 0.04	$(5.84 \pm 1.43) \times 10^5$
diphosphorylated	0.66 ± 0.30	0.02 ± 0.01	$(3.69 \pm 0.34) \times 10^4$
	96.6 ± 23.7	0.46 ± 0.06	$(4.96 \pm 1.46) \times 10^3$

[a] The hydrolysis of [^{3}H]Ap_3A by Fhit was measured as described in Experimental Procedures. Values are means $\pm$ the standard deviation ($n = 6$ assays) for each form of Fhit. Values for k_{cat} for the diphosphorylated Fhit were calculated assuming equal numbers of low- and high-K_m sites.

We previously reported a k_{cat} value of 73 s^{-1} for hydrolysis of Ap_3A by unphosphorylated Fhit (*15*). We now believe this value was high due to a systematic error in preparing serial dilutions of concentrated enzyme samples for the assay. Previously, the same pipet tip was used throughout the dilutions, flushing it repeatedly at each step. When a fresh tip was used at each step, the activity that was measured was lower, and the parameters that were obtained were more consistent between experiments. The k_{cat} value of 2.74 s^{-1} reported here (Table 1) is similar to values reported by other investigators (*17*, *24*, *35*).

DISCUSSION

Human Fhit can be phosphorylated in *E. coli* using a tyrosine-phosphorylating strain. In *E. coli*, Fhit is phosphorylated on Y^{114}, and only Y^{114}, exactly as Fhit is phosphorylated in vitro with Src kinase and ATP and in vivo in transfected NIH-3T3 mouse fibroblasts (*27*). Unphosphorylated Fhit was less than 10% of the phosphorylated forms in the in vitro reaction with Src kinase (*27*), whereas in the *E. coli* phosphorylation system, unphosphorylated Fhit is approximately equal to the amount of phosphorylated Fhit. Although the *E. coli* phosphorylation system is less efficient than the in vitro system with Src kinase, the bacterial systems allows purification of phosphorylated forms of Fhit in sufficient amounts for structural studies.

Fhit is a homodimer which can bind a molecule of substrate at each active site simultaneously (*15*) (Figure 6). It would be reasonable to expect biphasic kinetics in the monophosphorylated form and monophasic kinetics in the diphosphorylated form. The counterintuitive results suggest the possibility of novel enzymology.

Tyrosine 114 is within a 21-residue segment of Fhit (residues 107−127) which is invisible in all crystal structures obtained thus far, including those with a bound substrate analogue, product, or analogue of the covalent intermediate (*15*−*17*). The tyrosine is the most highly conserved residue in this loop. It is present in 19 of 20 species, being replaced only in *Candida albicans* by histidine (based on a search of GenBank in September 2004) (*36*) The proximal segment of the loop through L^{117} contains the only widely conserved residues in the loop and is conserved in length in Fhit orthologs at 9−10 residues. The downstream segment is 7−17 residues long in animal and plant Fhits, but 7−55 residues long in unicellular eukaryotes. The size and apparent flexibility of the loop suggest that it may able to affect the active site directly (Figure 6).

The fact that phosphorylation on only one subunit resulted in a greater than 50% loss of activity indicates that a single phosphorylated subunit can in fact inhibit both active sites. A phosphorylated Y^{114} might inhibit activity by the phosphate occupying some part of the substrate binding site, which would result in a high K_m. However, it is not clear why this would happen only when Y^{114} is phosphorylated on both subunits. Phosphorylation of only one Y^{114} might result in the complete inhibition of that subunit's active site as a result of the loop taking on a conformation that sterically obstructs it. One possibility would be bridging of the phosphate group to the R^{102} of the opposite subunit (Figure 6). Arginine−phosphate interactions are common in phosphorylated proteins (*37*). Concomitant with obstructing one active site, a conformational change induced by the phosphorylated Y^{114} in the remaining active site may result in altered kinetic parameters for the residual activity.

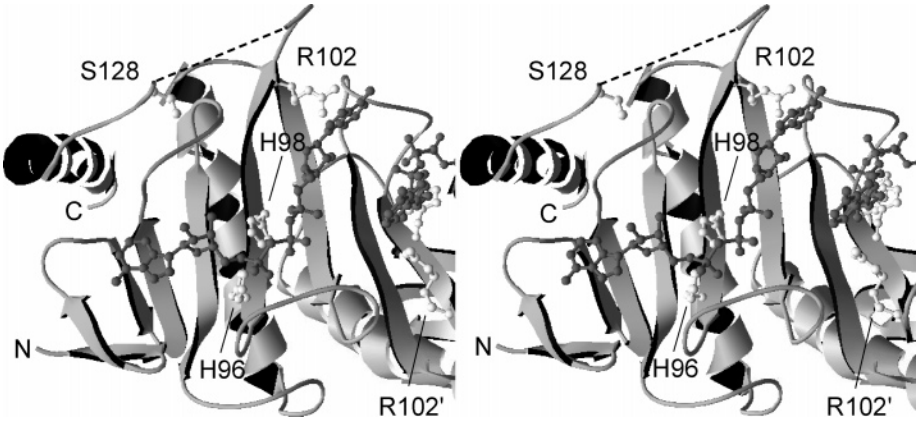

FIGURE 6: Stereo diagram of Fhit with a bound Ap_3A analogue. The substrate analogue is Ado-p-CH_2-p-p_s-Ado. The dotted line indicates the base of the invisible loop. S^{128} is the first residue resolved after the loop. The reaction center is marked by H^{96}, which forms a covalent intermediate at the α-phosphate of Ap_3A during the reaction, and H^{98}, which is necessary for full activity. The diagram is based on PDB entry 1FHI (*15*).

In the diphosphorylated enzyme, one must invoke either two different monomer conformations in the dimer or two different dimer forms, presumably in equilibrium. In the latter case, the k_{cat} values cannot be calculated without knowing the distribution of dimers between the two forms. The low-K_m phase may be similar to the monophosphorylated state, with one subunit's active site blocked, and the activity of the functioning active site perhaps further affected by the phosphate on that subunit. The high-K_m phase may result from symmetrical dimers in which both active sites are partially obstructed by the phosphorylated loops. In this case, biphasic kinetics would result from different dimers existing in different conformations. Some of these mechanisms are expected to result in fixing all or part of the loop(s) in one position in the phosphorylated protein. Sufficient amounts of phosphorylated Fhit are available to measure the mobility of the phosphorylated loop and, if it is fixed, to determine the protein structure.

Fhit is a tumor suppressor with the capacity to hydrolyze Ap_3A, yet its suppressor activity seems to be dependent only on binding Ap_3A or some related ligand. It has been proposed that the enzyme−substrate complex is the form that interacts with the apoptosis pathway (*15*, *26*). Phosphorylation decreased the values of K_m and k_{cat} for Ap_3A hydrolysis by monophosphorylated Fhit and by the low-K_m site in diphosphorylated Fhit. The decreases in values of K_m and k_{cat} for the phosphorylated forms in comparison to unphosphorylated Fhit favor the formation and lifetime of the Fhit−Ap_3A complex, which may enhance the tumor suppressor activity of Fhit. The phosphotyrosine itself may be a binding site for interacting proteins. The sequence surrounding the tyrosine is compatible with binding by an SH2 domain (*38*). Sufficient amounts of phosphorylated Fhit are available to test for interaction with potential target proteins relevant to its tumor suppressor activity.

ACKNOWLEDGMENT

We thank Dr. Susan Weintraub and Chris Carroll from the Center for Mass Spectrometry at the University of Texas Health Sceince Center for their assistance and expertise. The Center for Mass Spectrometry is supported by NCI Grant P30CA54174 through the San Antonio Cancer Institute. We thank the anonymous reviewers for useful suggestions. Preliminary results were presented at the American Society of Biochemistry and Molecular Biology annual meeting in Boston, MA, June 12−16, 2004.

REFERENCES

1. Ohta, M., Inoue, H., Cotticelli, M. G., Kastury, K., Baffa, R., Palazzo, J., Siprashvili, Z., Mori, M., McCue, P., Druck, T., Croce, C. M., and Huebner, K. (1996) The *FHIT* gene, spanning the chromosome 3p14.2 fragile site and renal carcinoma-associated t(3;8) breakpoint, is abnormal in digestive tract cancers, *Cell 84*, 587−597.
2. Matsuyama, A., Shiraishi, T., Trapasso, F., Kuroki, T., Alder, H., Mori, M., Huebner, K., and Croce, C. M. (2003) Fragile site orthologs FHIT/FRA3B and Fhit/Fra14A2: Evolutionarily conserved but highly recombinogenic, *Proc. Natl. Acad. Sci. U.S.A. 100*, 14988−14993.
3. Croce, C. M., Sozzi, G., and Huebner, K. (1999) Role of *FHIT* in human cancer, *J. Clin. Oncol. 17*, 1618−1624.
4. Huebner, K., Garrison, P. N., Barnes, L. D., and Croce, C. M. (1998) The role of the FHIT/FRA3B locus in cancer, *Annu. Rev. Genet. 32*, 7−31.
5. Huebner, K., Sozzi, G., Brenner, C., Pierotti, M. A., and Croce, C. M. (1999) Fhit loss in lung cancer: Diagnostic and therapeutic implications, *Adv. Oncol. 15*, 3−10.
6. Sozzi, G., Huebner, K., and Croce, C. M. (1998) *FHIT* in human cancer, *Adv. Cancer Res. 72*, 141−166.
7. Huebner, K., and Croce, C. M. (2003) Cancer and the FRA3B/FHIT fragile locus: It's a HIT, *Br. J. Cancer 88*, 1501−1506.
8. Siprashvili, Z., Sozzi, G., Barnes, L. D., McCue, P., Robinson, A. K., Eryomin, V., Sard, L., Tagliabue, E., Greco, A., Fusetti, L., Schwartz, G., Pierotti, M. A., Croce, C. M., and Huebner, K. (1997) Replacement of Fhit in cancer cells suppresses tumorigenicity, *Proc. Natl. Acad. Sci. U.S.A. 94*, 13771−13776.
9. Ji, L., Fang, B., Yen, N., Fong, K., Minna, J. D., and Roth, J. A. (1999) Induction of apoptosis and inhibition of tumorigenicity and tumor growth by adenovirus vector-mediated fragile histidine triad (FHIT) gene overexpression, *Cancer Res. 59*, 3333−3339.
10. Fong, L. Y., Fidanza, V., Zanesi, N., Lock, L. F., Siracusa, L. D., Mancini, R., Siprashvili, Z., Ottey, M., Martin, S. E., Druck, T., McCue, P. A., Croce, C. M., and Huebner, K. (2000) Muir-Torre-like syndrome in Fhit-deficient mice, *Proc. Natl. Acad. Sci. U.S.A. 97*, 4742−4747.
11. Dumon, K. R., Ishii, H., Fong, L. Y., Zanesi, N., Fidanza, V., Mancini, R., Vecchione, A., Baffa, R., Trapasso, F., During, M. J., Huebner, K., and Croce, C. M. (2001) FHIT gene therapy prevents tumor development in Fhit-deficient mice, *Proc. Natl. Acad. Sci. U.S.A. 98*, 3346−3351.
12. Ishii, H., Zanesi, N., Vecchione, A., Trapasso, F., Yendamuri, S., Sarti, M., Baffa, R., During, M. J., Huebner, K., Fong, L. Y., and Croce, C. M. (2003) Regression of upper gastric cancer in mice by FHIT gene delivery, *FASEB J. 17*, 1768−1770.

13. Sard, L., Accornero, P., Tornielli, S., Delia, D., Bunone, G., Campiglio, M., Colombo, M. P., Gramegna, M., Croce, C. M., Pierotti, M. A., and Sozzi, G. (1999) The tumor-suppressor gene FHIT is involved in the regulation of apoptosis and in cell cycle control, *Proc. Natl. Acad. Sci. U.S.A. 96*, 8489−8492.
14. Roz, L., Gramegna, M., Ishii, H., Croce, C. M., and Sozzi, G. (2002) Restoration of fragile histidine triad (FHIT) expression induces apoptosis and suppresses tumorigenicity in lung and cervical cancer cell lines, *Proc. Natl. Acad. Sci. U.S.A. 99*, 3615−3620.
15. Pace, H. C., Garrison, P. N., Robinson, A. K., Barnes, L. D., Draganescu, A., Rösler, A., Blackburn, G. M., Siprashvili, Z., Croce, C. M., Huebner, K., and Brenner, C. (1998) Genetic, biochemical, and crystallographic characterization of Fhit-substrate complexes as the active signaling form of Fhit, *Proc. Natl. Acad. Sci. U.S.A. 95*, 5484−5489.
16. Lima, C. D., D'Amico, K. L., Naday, I., Rosenbaum, G., Westbrook, E. M., and Hendrickson, W. A. (1997) MAD analysis of FHIT, a putative human tumor suppressor from the HIT protein family, *Structure 5*, 763−774.
17. Lima, C. D., Klein, M. G., and Hendrickson, W. A. (1997) Structure-based analysis of catalysis and substrate definition in the HIT protein family, *Science 278*, 286−290.
18. Brenner, C. (2002) Hint, Fhit, and GalT: Function, structure, evolution, and mechanism of three branches of the histidine triad superfamily of nucleotide hydrolases and transferases, *Biochemistry 41*, 9003−9014.
19. Huang, Y., Garrison, P. N., and Barnes, L. D. (1995) Cloning of the *Schizosaccharomyces pombe* gene encoding diadenosine 5′,5‴-P^1,P^4-tetraphosphate (Ap_4A) asymmetrical hydrolase: Sequence similarity with the histidine triad (HIT) protein family, *Biochem. J. 312*, 925−932.
20. Barnes, L. D., Garrison, P. N., Siprashvili, Z., Guranowski, A., Robinson, A. K., Ingram, S. W., Croce, C. M., Ohta, M., and Huebner, K. (1996) Fhit, a putative tumor suppressor in humans, is a dinucleoside 5′,5‴-P^1,P^3-triphosphate hydrolase, *Biochemistry 35*, 11529−11535.
21. Chen, J., Brevet, A., Blanquet, S., and Plateau, P. (1998) Control of 5′,5′-dinucleoside triphosphate catabolism by APH1, a *Saccharomyces cerevisiae* analog of human FHIT, *J. Bacteriol. 180*, 2345−2349.
22. Pekarsky, Y., Campiglio, M., Siprashvili, Z., Druck, T., Sedkov, Y., Tillib, S., Draganescu, A., Wermuth, P., Rothman, J. H., Huebner, K., Buchberg, A. M., Mazo, A., Brenner, C., and Croce, C. M. (1998) Nitrilase and Fhit homologs are encoded as fusion proteins in *Drosophila melanogaster* and *Caenorhabditis elegans*, *Proc. Natl. Acad. Sci. U.S.A. 95*, 8744−8749.
23. Abend, A., Garrison, P. N., Barnes, L. D., and Frey, P. A. (1999) Stereochemical retention of the configuration in the action of Fhit on phosphorus-chiral substrates, *Biochemistry 38*, 3668−3676.
24. Huang, K., Arabshahi, A., Wei, Y., and Frey, P. A. (2004) The mechanism of action of the fragile histidine triad, Fhit: Isolation of a covalent adenylyl enzyme and chemical rescue of H96G-Fhit, *Biochemistry 43*, 7637−7642.
25. Werner, N. S., Siprashvili, Z., Fong, L. Y., Marquitan, G., Schroder, J. K., Bardenheuer, W., Seeber, S., Huebner, K., Schutte, J., and Opalka, B. (2000) Differential susceptibility of renal carcinoma cell lines to tumor suppression by exogenous Fhit expression, *Cancer Res. 60*, 2780−2785.
26. Trapasso, F., Krakowiak, A., Cesari, R., Arkles, J., Yendamuri, S., Ishii, H., Vecchione, A., Kuroki, T., Bieganowski, P., Pace, H. C., Huebner, K., Croce, C. M., and Brenner, C. (2003) Designed FHIT alleles establish that Fhit-induced apoptosis in cancer cells is limited by substrate binding, *Proc. Natl. Acad. Sci. U.S.A. 100*, 1592−1597.
27. Pekarsky, Y., Garrison, P. N., Palamarchuk, A., Zanesi, N., Aqeilan, R. I., Huebner, K., Barnes, L. D., and Croce, C. M. (2004) Fhit is a physiological target of the protein kinase Src, *Proc. Natl. Acad. Sci. U.S.A. 101*, 3775−3779.
28. Brenner, C., Pace, H. C., Garrison, P. N., Robinson, A. K., Rosler, A., Liu, X. H., Blackburn, G. M., Croce, C. M., Huebner, K., and Barnes, L. D. (1997) Purification and crystallization of complexes modeling the active state of the fragile histidine triad protein, *Protein Eng. 10*, 1461−1463.
29. Ghosh, S., and Lowenstein, J. M. (1996) A multifunctional vector system for heterologous expression of proteins in *Escherichia coli*. Expression of native and hexahistidyl fusion proteins, rapid purification of the fusion proteins, and removal of fusion peptide by Kex2 protease, *Gene 176*, 249−255.
30. Laemmli, U. K. (1970) Cleavage of structural proteins during the assembly of the head of bacteriophage T4, *Nature 227*, 680−685.
31. Studier, F. W. (1973) Analysis of bacteriophage T7 early RNAs and proteins on slab gels, *J. Mol. Biol. 79*, 237−248.
32. Lee, T. D., and Shively, J. E. (1990) Enzymatic and chemical digestion of proteins for mass spectrometry, *Methods Enzymol. 193*, 361−374.
33. Barnes, L. D., Robinson, A. K., Mumford, C. H., and Garrison, P. N. (1985) Assay of diadenosine tetraphosphate hydrolytic enzymes by boronate chromatography, *Anal. Biochem. 144*, 296−304.
34. Lee, H. J., and Wilson, I. B. (1971) Enzymic parameters: Measurement of V and K_m, *Biochim. Biophys. Acta 242*, 519−522.
35. Golebiowski, F., Szulc, A., Szutowicz, A., and Pawelczyk, T. (2004) Ubc9-induced inhibition of diadenosine triphosphate hydrolase activity of the putative tumor suppressor protein Fhit, *Arch. Biochem. Biophys. 428*, 160−164.
36. Jeanmougin, F., Thompson, J. D., Gouy, M., Higgins, D. G., and Gibson, T. J. (1998) Multiple sequence alignment with Clustal X, *Trends Biochem. Sci. 23*, 403−405.
37. Johnson, L. N., and Lewis, R. J. (2001) Structural basis for control by phosphorylation, *Chem. Rev. 101*, 2209−2242.
38. Obenauer, J. C., Cantley, L. C., and Yaffe, M. B. (2003) Scansite 2.0: Proteome-wide prediction of cell signaling interactions using short sequence motifs, *Nucleic Acids Res. 31*, 3635−3641.

BI047670S